

# Anomalously high $b$ -values in the South Flank of Kilauea volcano, Hawaii: evidence for the distribution of magma below Kilauea's East rift zone

M. Wyss<sup>a,\*</sup>, F. Klein<sup>b</sup>, K. Nagamine<sup>c</sup>, S. Wiemer<sup>d</sup>

<sup>a</sup>Geophysical Institute, University of Alaska, Fairbanks, AK 99775, USA

<sup>b</sup>US Geological Survey, Menlo Park, CA 94025, USA

<sup>c</sup>Graduate School of Human Informatics, Nagoya University, Chikusa, Nagoya 464-8601, Japan

<sup>d</sup>Institut fuer Geophysik, ETH Hoenggerberg, 8093 Zuerich, Switzerland

Received 11 May 2000; accepted 2 October 2000

## Abstract

The pattern of  $b$ -value of the frequency–magnitude relation, or mean magnitude, varies little in the Koaiki-Hilea area of Hawaii, and the  $b$ -values are normal, with  $b = 0.8$  in the top 10 km and somewhat lower values below that depth. We interpret the Koaiki-Hilea area as relatively stable, normal Hawaiian crust. In contrast, the  $b$ -values beneath Kilauea's South Flank are anomalously high ( $b = 1.3$ – $1.7$ ) at depths between 4 and 8 km, with the highest values near the East Rift zone, but extending 5–8 km away from the rift. Also, the anomalously high  $b$ -values vary along strike, parallel to the rift zone. The highest  $b$ -values are observed near Hiiaka and Pauahi craters at the bend in the rift, the next highest are near Makaopuhi and also near Puu Kaliu. The mildest anomalies occur adjacent to the central section of the rift. The locations of the three major and two minor  $b$ -value anomalies correspond to places where shallow magma reservoirs have been proposed based on analyses of seismicity, geodetic data and differentiated lava chemistry. The existence of the magma reservoirs is also supported by magnetic anomalies, which may be areas of dike concentration, and self-potential anomalies, which are areas of thermal upwelling above a hot source. The simplest explanation of these anomalously high  $b$ -values is that they are due to the presence of active magma bodies beneath the East Rift zone at depths down to 8 km. In other volcanoes, anomalously high  $b$ -values correlate with volumes adjacent to active magma chambers. This supports a model of a magma body beneath the East Rift zone, which may widen and thin along strike, and which may reach 8 km depth and extend from Kilauea's summit to a distance of at least 40 km down rift. The anomalously high  $b$ -values at the center of the South Flank, several kilometers away from the rift, may be explained by unusually high pore pressure throughout the South Flank, or by anomalously strong heterogeneity due to extensive cracking, or by both phenomena. The major  $b$ -value anomalies are located SSE of their parent reservoirs, in the direction of motion of the flank, suggesting that magma reservoirs leave an imprint in the mobile flank. We hypothesize that the extensive cracking may have been acquired when the anomalous parts of the South Flank, now several kilometers distant from the rift zone, were generated at the rift zone near persistent reservoirs. Since their generation, these volumes may have moved seaward, away from the rift, but earthquakes occurring in them still use the preexisting complex crack distribution. Along the decollement plane at 10 km depth, the  $b$ -values

\* Corresponding author. Fax: +1-907-474-7290.

E-mail addresses: max@giseis.alaska.edu (M. Wyss), klein@usgs.gov (F. Klein), nagamine@info.human.nagoya-u.ac.jp (K. Nagamine), stefan@seismo.ifg.ethz.ch (S. Wiemer).

are exceptionally low ( $b = 0.5$ ), suggesting faulting in a more homogeneous medium. © 2001 Elsevier Science B.V. All rights reserved.

*Keywords:* magma;  $b$ -value; frequency–magnitude; volcanic seismicity

## 1. Introduction

The island of Hawaii is built upon the ocean floor by magmatic intrusive and extrusive material (Hill and Zucca, 1987). As the ocean floor moves over the hot spot, older volcanoes (Mauna Kea) are disconnected from the magma supply and new volcanoes (Loihi) are created. For this reason, the magma plumbing system under Hawaii may be expected to be more complex (Ryan, 1988) than under single volcanoes that remain above their magma supply for long periods. In such a case of strong complexity it is of special interest, but perhaps also more difficult than usual, to map the conduits and chambers containing magma. In this paper, we use the frequency magnitude distribution (FMD) of earthquakes to infer the presence of magma, concentrating on Kilauea's South Flank and in the Kaoiki-Hilea region between Mauna Loa and Kilauea. Because our method is based on seismicity, we can extract information only from parts of the crust and upper mantle that produce numerous earthquakes. In Hawaii, most seismic activity is concentrated in the

volcanic edifice that rests on the depressed oceanic sea floor.

The crustal volumes beneath the South Flank and Kaoiki produce abundant earthquakes (Fig. 1), mostly at depths between 4 and 10 km within the volcanic edifice (Fig. 2). The earthquakes in these volumes are thought to be volcano-tectonic in the sense that they are generated by stresses exerted by the volcanoes and their rifts, but not directly related to opening of magmatic conduits or the flow of magma. The distances of the epicenters from the rift zones and the calderas range from about 1–10 km. The largest recent earthquakes were an  $M6.6$  in 1983 and an  $M6.1$  in 1989 in the Kaoiki and South Flank areas, respectively. However, both areas are underlain by a near horizontal decollement plane, the surface of the old sea floor, which can generate large to great earthquakes (Wyss, 1988). In 1975, an  $M7.2$  earthquake ruptured most of the decollement plane under the South Flank (Swanson et al., 1976b), and in 1868, a  $M7.9$  earthquake probably ruptured all of the South Flank, Kaoiki, Hilea and adjacent areas (Wyss, 1988).

Along Kilauea's east- and southwest rift zones,

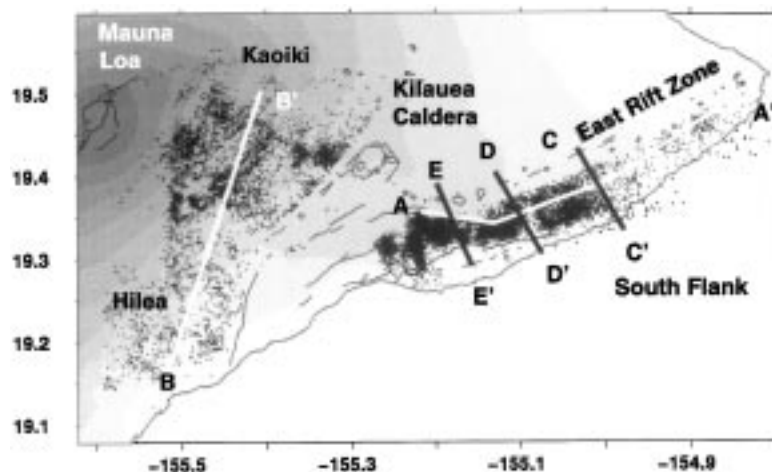


Fig. 1. Epicenter map for the study areas in Southern Hawaii. Only epicenters in the Kaoiki-Hilea area and Kilauea's South Flank are used, avoiding rift zones, calderas and other known magma supply routes. The coastline, calderas and rift zones are outlined. The position of cross sections shown in Figs. 4 and 5 are defined.

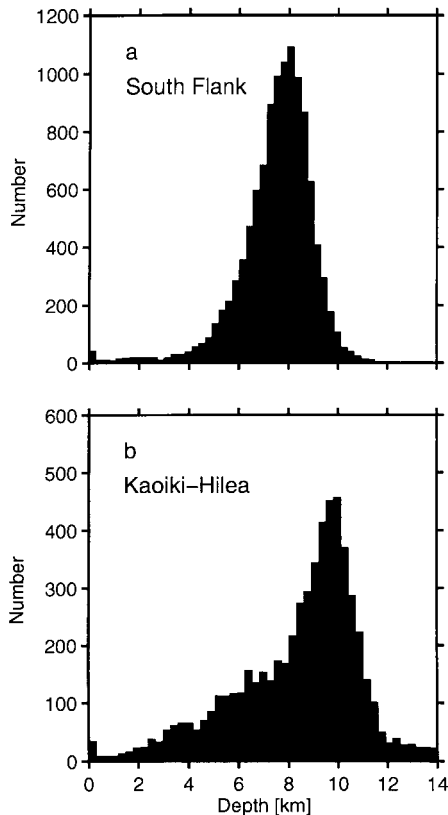


Fig. 2. Numbers of earthquakes with  $M \geq 1.5$  as a function of depth for: (a) Kilauea's South Flank; and (b) the Kaoiki-Hilea region.

large numbers of small earthquakes occur during magmatic intrusions (Dvorak et al., 1986). These intrusions often initiate under Kilauea's caldera (Dzurisin et al., 1984; Klein et al., 1987), propagate down the rift zones, generate varying degrees of seismicity, and in many cases end up in eruptions from a subsidiary cone in the rift zone (Hardee, 1987). The seismic activity during rift intrusions occurs primarily between 2 and 4 km depth and follows closely the surface trace of the rift. Because of this, most early models of the east rift zone envisioned the active zone to exist down to 4 or 6 km. However, a model with magma bodies down to 10 km depth beneath the rift zones (Crosson and Endo, 1982; Ryan, 1988) received support from geodetic data (Delaney et al., 1990), which required an expanding magma body at 3–9 km depth to satisfactorily explain the surface deformations. In this paper we present data from the

frequency–magnitude relation of earthquakes beneath the South Flank that support the model of magma bodies beneath the East Rift zone that may reach depths of 8 km. The data also suggest that the greatest effect on the South Flank earthquake magnitude distribution occurs at intermediate depths (4–7 km) adjacent to shallow (2–4 km) magma bodies under the rift that have been proposed based on analysis of deformation, lava chemistry and seismicity patterns. We do not analyze the seismicity of the rift zone itself because the earthquakes in it occur primarily during intrusions of magma, have a complicated time–space history and carry no information about crustal conditions in the South Flank.

The relative abundance of small earthquakes compared to large ones is measured by the  $b$ -value in the FMD (Ishimoto and Iida, 1939; Gutenberg and Richter, 1944)

$$\log N = a - bM \quad (1)$$

where  $N$  is the cumulative number of earthquakes with magnitude  $M$  and larger.

A number of recent papers demonstrated that the constants  $a$  and  $b$  vary strongly over a few kilometers distance in seismogenic volumes (Ogata et al., 1995; Wiemer and Benoit, 1996; Wiemer and McNutt, 1997; Wiemer and Wyss, 1997; Wyss et al., 1997; Wiemer et al., 1998; Power et al., 1998; Murru et al., 1999; Wiemer and Katsumata, 1999). This means that the mean magnitude,  $m$ , varies as a function of space because the  $b$ -value is inversely proportional to the mean magnitude (Aki, 1965; Utsu, 1965)

$$m = M_{\min} + 1/2.3b \quad (2)$$

In this paper, we map  $m$ . We do not assume that the FMD is approximated well by a power law, nor do we make any extrapolations based on a straight line fit. Therefore, it is inconsequential if the straight line fit may not be a good approximation in some volumes, because we are simply comparing the mean magnitude in different volumes by mapping the  $b$ -value.

Along the San Andreas fault system, creeping segments show anomalously high values ( $b > 1.3$ ) (Amelung and King, 1997; Wiemer and Wyss, 1997), whereas asperities correlate with anomalously low values ( $b < 0.6$ ) (Wiemer and Wyss, 1997; Wyss et al., 1999). In general, the  $b$ -values decrease with

depth in California (Mori and Abercrombie, 1997; Wiemer and Wyss, 1997; Wiemer et al., 1998; Gerstenberger et al., 2000). In aftershock sequences, great variability of  $b$ -values is possibly related to the amount of slip during the main shock (Wiemer and Katsumata, 1999). Beneath volcanoes, the volumes surrounding active magma chambers and conduits exhibit anomalously high  $b$ -values (Wiemer and McNutt, 1997; Wyss et al., 1997; Wiemer et al., 1998; Murru et al., 1999).

We know from laboratory experiments, observations in underground mines and near wells that the  $b$ -value increases with decreasing effective stress, and with increasing heterogeneity of the material (Mogi, 1962; Scholz, 1968; Wyss, 1973; Urbancic et al., 1992), and that it may also be sensitive to the temperature gradient (Warren and Latham, 1970). A recent study by Lahaie and Grasso (1999) showed a correlation between the loading rate and the  $b$ -value at the Lacq gas field in France: When the loading rate was reduced, the  $b$ -value increased by almost a factor of two.

We interpreted the low  $b$ -values in asperities as expressions of elevated stress levels. The anomalously high  $b$ -values near magma chambers can be explained as due to larger-than-normal heterogeneity, or, alternatively, as due to high pore pressure. The purpose of this paper is to map the distribution of  $b$ -values in Kilauea's South Flank and in the Kaoiki-Hilea area, and to construct a model for the generation of the related earthquakes.

## 2. Data

The newest version of the Hawaiian Volcano Observatory's earthquake catalog was used to estimate the mean magnitude ( $b$ -value). Among the several magnitudes available, we have most confidence in the homogeneity of the 'preferred magnitude' ( $M_p$ ) because this magnitude furnishes stable  $b$ -value estimates and it is available for the largest number of earthquakes.  $M_p$  is selected by a hierarchical scheme defined in the data description prepared by F. Klein for distribution of the Hawaiian earthquake catalog. The preferred magnitude  $M_p$  is  $M_S$  for the few cases where it is available,  $M_L$  when it is larger than 1.99, and in other cases is the duration

magnitude  $M_D$ . The definition of  $M_p$  was introduced before this study and is completely independent from the goals of this study.

Because we have discovered that in some catalogs the magnitude scale was inadvertently shifted or stretched at times (Zuniga and Wyss, 1995; Zuniga and Wiemer, 1999), we searched the Hawaiian catalog for such problems. Changes in reporting, identified by the computer algorithm GENAS (Habermann, 1983), were examined by comparing the FMD plots before and after the change. Then the transformation equation of the old to the new magnitude scale was calculated (Zuniga and Wyss, 1995), all using the software ZMAP (Wiemer and Zuniga, 1994). In the  $M_p$  data, the strongest change was a magnitude shift of  $-0.5$  in 1984. The shift was constant for all magnitude bands. Thus, the  $b$ -values of the old and new scales remained unchanged. After 1991, when the Wood-Anderson seismometers were disconnected, more heterogeneity was present than before. Thus, we used the  $M_p$  for the period 1979–1991, with a correction for the magnitude shift in 1984. All the figures shown here are based on analysis of  $M_p$ .

However, in order to ascertain that the results do not depend on the choice of magnitude, nor the correction for the data after 1984, we also performed the analysis using  $M_d$ . The duration magnitude,  $M_d$ , is the second-most commonly available magnitude estimate. It is not available for the years 1990–1992.5, but has otherwise been reported fairly consistently during the period 1979–1997. In this case, we accepted all data uncorrected for the years 1989–1997. These were 6.5 years of data, since  $M_d$  has not been computed for 1990–1992.5. The resulting figures resemble very closely the figures presented in this paper, which are based on the  $M_p$ .

In the data set of  $M_p$ , the average minimum magnitude of completeness was 1.5; in the case of  $M_d$ , it was 1.8. The difference is because the two magnitude scales are not identical. The total numbers of events above these minimum magnitudes were  $N(M_p)_{\text{tot}} = 16,963$  and  $N(M_d)_{\text{tot}} = 21,390$ . They were divided into  $N(M_p)_{\text{ka0}} = 5885$  and  $N(M_d)_{\text{ka0}} = 7803$  in the Kaoiki-Hilea area, versus  $N(M_p)_{\text{sf}} = 11,073$  and  $N(M_d)_{\text{sf}} = 13,587$  in the South Flank.

The hypocenters in the earthquake catalog covering the area of southern Hawaii are calculated from records of a seismograph network with about 35

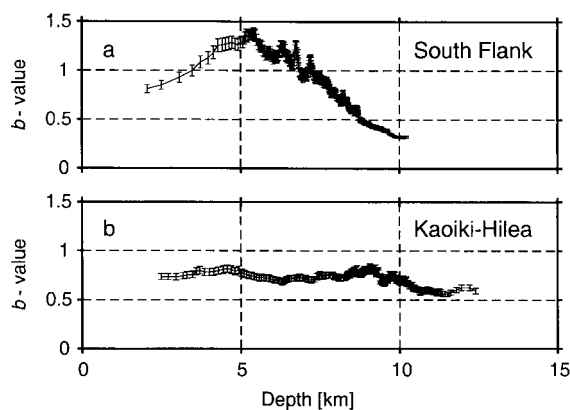


Fig. 3.  $b$ -values of the frequency-magnitude distribution as a function of depth for: (a) Kilauea's South Flank; and (b) the Kaoiki-Hilea region. The number of events ( $M \geq 1.5$ ) per window is 300. The Kaoiki-Hilea area shows normal to low values throughout the crust with a slight decrease as a function of depth, similar to the pattern observed in California. In contrast, the  $b$ -values in the South Flank of Kilauea are normal at shallow depths, increase to anomalously high values at intermediate depths and then plunge to anomalously low values at the depth of the decollement plain of 9 km.

stations within a radius of 30 km from Kilauea (Klein et al., 1987). The crustal model to locate earthquakes was derived by Klein (1981). The epicenters and depth estimates are believed to be accurate within 1 and 1.5 km, respectively. When hypocenters were relocated by special techniques, they contracted onto a plane, moving typically 1 km (Got et al., 1994; Gillard et al., 1996). This supports the above estimate of the hypocenter inaccuracies in the catalog we used. The earthquake catalog of Hawaii is therefore one of the most accurate data sets related to an active volcano. Another advantage of the data for the South Flank is that they do not contain any long period or other volcanic events that might contaminate the FMD of the volcano-tectonic earthquakes.

The epicenters of the earthquakes used are shown in Fig. 1. We selected earthquakes only in the central and eastern part of Kilauea's South Flank, as well as in the Kaoiki and the Hilea areas. Earthquakes located beneath the caldera, SW of it and along the rift zones were excluded from this study. The separation was naturally defined because there exists an aseismic band of crust along the rift zones.

The overall distribution of earthquakes as a func-

tion of depth is shown in Fig. 2 separately for the South Flank and the Kaoiki-Hilea areas. Few earthquakes occur at depths shallower than 4 km. Their numbers increase with depth, reach a peak at about 8–10 km, and then rapidly fall off to almost no events deeper than 10 and 12 km in the South Flank and Kaoiki, respectively.

### 3. Method

We estimate the mean magnitude, or  $b$ -value, by both the maximum likelihood and the least squares method at every node of grids with spacing of 1 km or less (Wiemer, 1996). At each node, we extract the nearest  $N$  events ( $50 < N < 300$ , but typically  $N = 100$ ) to estimate  $b$ . The radii of the cylindrical volumes that contain 100 events are typically  $r = 1, 1.5$  and 3 km on the South Flank, in Kaoiki and in Hilea, respectively, but they vary inversely proportional to the local seismicity rate. From the resulting  $b$ -value maps and cross sections, we can then identify areas of anomalously low or high  $b$ -values and compare their earthquake populations to areas of normal distribution.

We estimate the minimum magnitude of completeness,  $M_c$ , for the overall sample, but also as a function of space and time. First, we cull the data, retaining events larger than the overall  $M_c$  that is approximately valid for the entire observation period. In addition, we estimate the local minimum magnitude of completeness,  $M_{loc}$ , for every sample processed by algorithm (Wiemer et al., 1998). This procedure minimizes the possibility of incorrect  $b$ -value estimates by the algorithm. The quality of the automatic  $b$ -value estimates was spot-checked by the authors. The overall minimum magnitude retained in the catalog for study was  $M_c = 1.5$ . For earthquakes above 7 km,  $M_{loc} = 1.7$  in the Hilea area and 1.8 in the eastern part of the South Flank. For earthquakes below 7 km,  $M_{loc}$  rises to 1.9 in some areas.

The  $b$ -value maps and cross sections shown are all based on the maximum likelihood estimate of the mean magnitude. However, we verified that the results are not significantly different when we use the weighted least squares fit to estimate  $b$ .

The statistical significance of differences between  $b$ -values in different volumes is estimated using

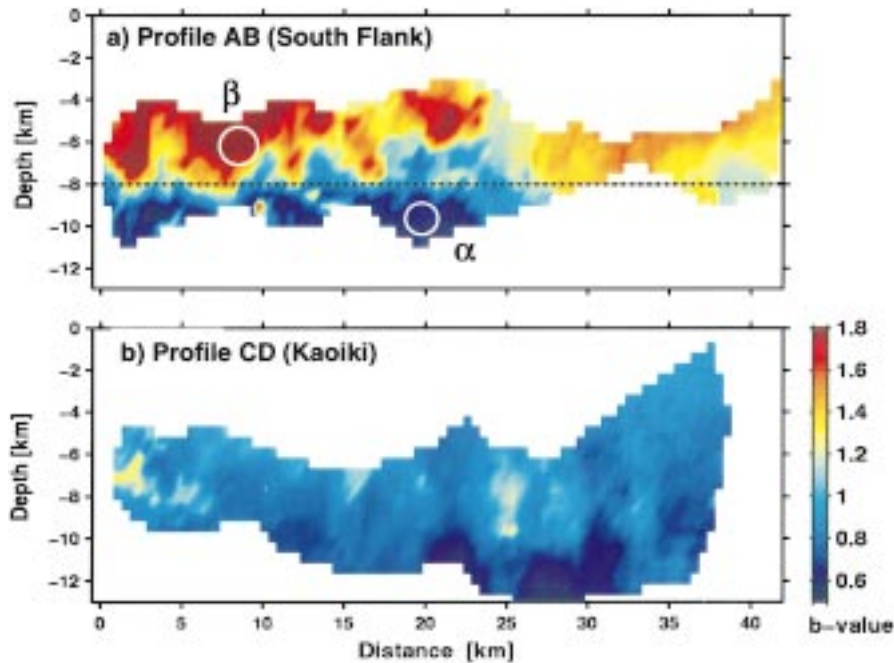


Fig. 4. Cross sections 10 km wide of  $b$ -values on grids with 1 km nodal spacing for: (a) Kilauea's South Flank parallel to the strike of the rift and the coast; and (b) the Kaoiki-Hilea region. Positions of cross sections are defined in Fig. 1.  $N = 150$  at each node. Anomalously high  $b$ -values are seen at intermediate depths in Kilauea's South Flank only.

Utsu's test (Utsu, 1992), which is valid for randomly selected samples (see our previous papers for equation and discussion, (Wyss et al., 1997)). This approach accounts for the uncertainties in both samples and directly furnishes the information of interest here, the confidence level with which a difference is established.

Because there is a question whether it is better to use the entire catalog or the declustered part (no aftershocks and swarms) for mapping  $b$ -values, we performed the analysis using both data sets. Reasenber's Reasenber (1985) algorithm with the original parameters was used to decluster. The declustered data showed all the essential features, including the duplication of some of the details. However, the reduction in numbers in the declustered catalog led to a lack of information in some volumes. (For example, in Fig. 5b the  $b$ -values could not be mapped for depths shallower than 4 km.) Given that the differences were minor, and that there was more information in the complete catalog, we used the entire catalog for the figures.

#### 4. Analysis of mean magnitude

##### 4.1. Average $b$ -value as a function of depth

The average  $b$ -value is estimated as a function of depth by a moving sample window of  $N = 300$  events, starting with the 300 shallowest earthquakes and moving the window deeper in steps of 10 events (Fig. 3). In the Kaoiki-Hilea area, the  $b$ -value remains approximately constant ( $b = 0.8$ ) down to about 10 km depth, below which it decreases slightly (Fig. 3b). This is similar to the pattern observed along parts of the San Andreas fault (Eaton et al., 1970; Wyss, 1973; Mori and Abercrombie, 1997; Wiemer and Wyss, 1997; Gerstenberger et al., 2000), except that in California the decrease to lower  $b$ -values occurs at shallower depths. The value of  $b = 0.8$  in the Kaoiki-Hilea area is normal to low. The pattern of  $b$ -values as a function of depth in the Kaoiki-Hilea area is that expected for a normal tectonically active crust.

In the South Flank, the  $b$ -value pattern as a function of depth is radically different than that observed in the Kaoiki-Hilea area or in California. Normal  $b$ -values of

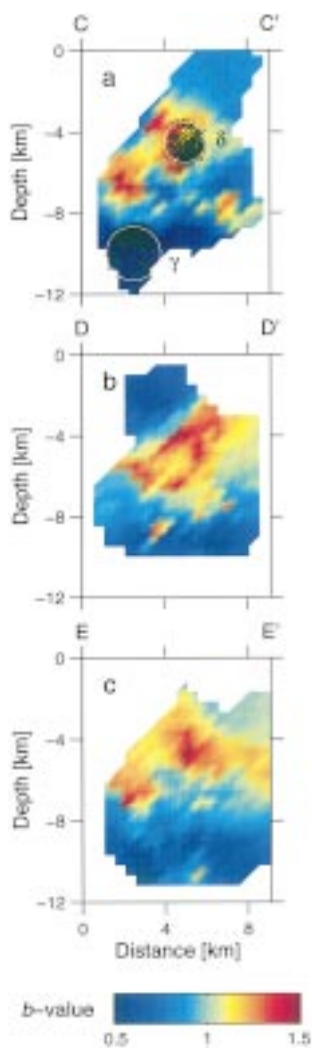


Fig. 5. Cross sections of  $b$ -values on grids with 1 km nodal spacing for the three sections perpendicular to the strike of the east rift in Kilauea's South Flank defined in Fig. 1.  $N = 100$  at each node. Circles define volumes for which the frequency–magnitude relations are shown in Fig. 7. All cross sections show anomalously high  $b$ -values at intermediate depths, but low  $b$ -values below 8 km, the location of the decollement plain.

about  $b = 0.8$ – $1.0$  are observed in the top 4 km, then they rise to  $b = 1.3$  at 6 km depth, below which they decline, especially below  $h = 8$  km, to anomalously low values of  $b = 0.4$  at 10 km depth (Fig. 3a). This is an unusual pattern not seen before away from volcanoes (Gerstenberger et al., 2000). Thus, a special explanation is needed for this observation.

#### 4.2. $b$ -Values in cross sections

We project the hypocenters of earthquakes in the South Flank onto a vertical plane oriented parallel to the coastline, and estimate the  $b$ -value at every node of a grid with 0.5 km spacing (Fig. 4a). The volumes sampled are cylinders with horizontal axes perpendicular to the cross section. This figure shows a clear difference of low  $b$ -values at depths deeper than 8 km, and high  $b$ -values at intermediate depth ( $3 > h > 7$  km). We interpret the low  $b$ -values near the bottom of the seismogenic layer as due to material homogeneity near the decollement plane with only one fault plane available for sliding. The cross section of the Koaiki-Hilea area does not show such a dependence of  $b$  with depth (Fig. 4b). Only a slight decrease below 10 km depth, as expected from Fig. 3b, can be discerned.

In three cross sections through the South Flank perpendicular to the East Rift zone, one again clearly sees the difference between low  $b$ -values below and high values above 8 km depth. We find that the anomalies at intermediate depths are most pronounced in the NW, in the crustal volumes closest to the rift zone (Fig. 5).

#### 4.3. $b$ -Values in map view

We constructed  $b$ -value maps for different depth ranges (Fig. 6) because of the pronounced dependence of  $b$  on depth, noticed in Figs. 3a and 4a for the South Flank. The anomalously high  $b$ -values for the intermediate depth range in the South Flank stand out clearly as red colors in Fig. 6a. The deepest section of the South Flank shows the darkest blue, corresponding to the anomalously low  $b$ -values already noticed in Figs. 3a and 4a for earthquakes near 10 km depth beneath the South Flank. Also, one can see that the volumes farthest removed from the East Rift zone tend to be less anomalous than those closer to it.

#### 4.4. Examples of frequency–magnitude distributions

It is important to verify that the contrasts in  $b$ -values mapped in Figs. 4–6 by algorithm are real, and that the  $M_{loc}$  chosen by the algorithm is acceptable, based on subjective examination of the FMD. We frequently examine FMDs for nodes in locations of

interest and in random locations during our analysis. In Fig. 7, we show examples of FMDs, comparing different volumes. In each frame the probability,  $P$ , that the two samples come from the same population is estimated based on the assumption that the samples are randomly selected (Utsu, 1992). The total number of events,  $n$ , and the  $b$ -value used for the probability estimates is given for each data set in Fig. 7.

The examples of contrasting FMDs show that extraordinarily strong differences exist between FMDs from different volumes, and that the  $M_{loc}$  defined by the algorithm are acceptable (Fig. 7). Although the data sets containing larger earthquakes (low  $b$ -values in Fig. 7) do not show the ideal straight-line distributions, it is clear that the earthquake population in these

volumes contrasts strongly with those in the volumes with high  $b$ -values. The latter never produced an earthquake with  $M > 2.6$  during the entire 14-year period covered by the catalog. This is anomalous and must represent a significant difference in the earthquake generation process or the tectonic environment in the contrasting crustal volumes.

The probabilities that the two samples compared in Figs. 7a and b, respectively, are from the same population with one common  $b$ -value are  $1.5 \cdot 10^{-11}$  and  $1.5 \cdot 10^{-9}$ . Once the  $b$ -values are mapped using our technique, such stark contrasts are not difficult to find. We do not discuss the uncertainties of the individual estimates of  $b$  because these are not of interest by themselves. The question of interest is at what level of

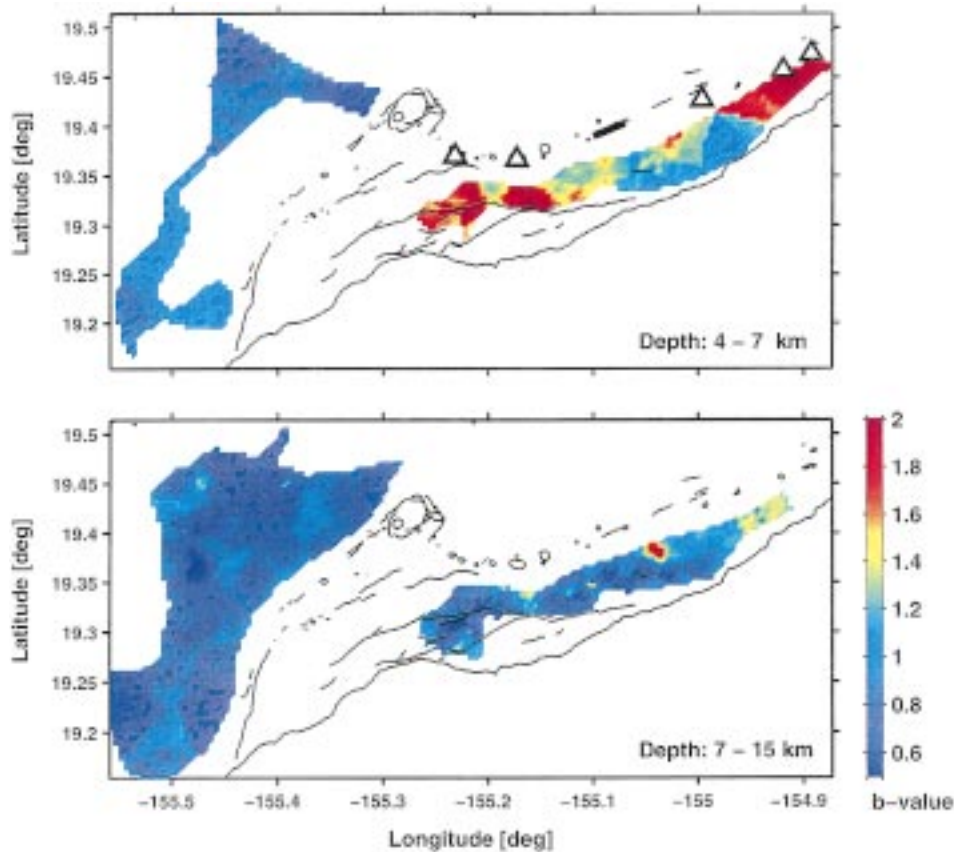


Fig. 6.  $b$ -value maps for Kilauea's South Flank and the Kaoiki-Hilea region for: (a) intermediate; and (b) deeper crustal earthquakes. The grid spacing is 0.5 km and  $N = 100$ . Normal to low values are typical for the Kaoiki-Hilea area, whereas anomalously high values are found at intermediate depth in Kilauea's South Flank. Pink triangles mark the locations of the shallow magma reservoirs estimated by independent data, and a heavy bar shows the segment of the rift over which another shallow magma reservoir is inferred to extend. Solid frames of four triangles mark the reservoirs which have an associated magnetic and/or a self-potential anomaly, and may represent the most persistent reservoirs.

confidence the Utsu (1992) test lets us accept the contention that the two samples are different. The degree of difference between red and blue areas in the maps and cross sections is generally on the level of the differences shown in Fig. 7. These differences are highly significant.

The three-dimensional image of the  $b$ -values beneath Kilauea's South Flank and the Kaoiki-Hilea areas shows the strong contrast at intermediate depths between the two crustal volumes (Fig. 8). The difference between  $b$ -values deeper than about 8 km and shallower in the South Flank is also very striking. In this image, no earthquakes from the rift zones or below the caldera were used. The intensity of the  $b$ -value anomalies varies along the rift, as is also

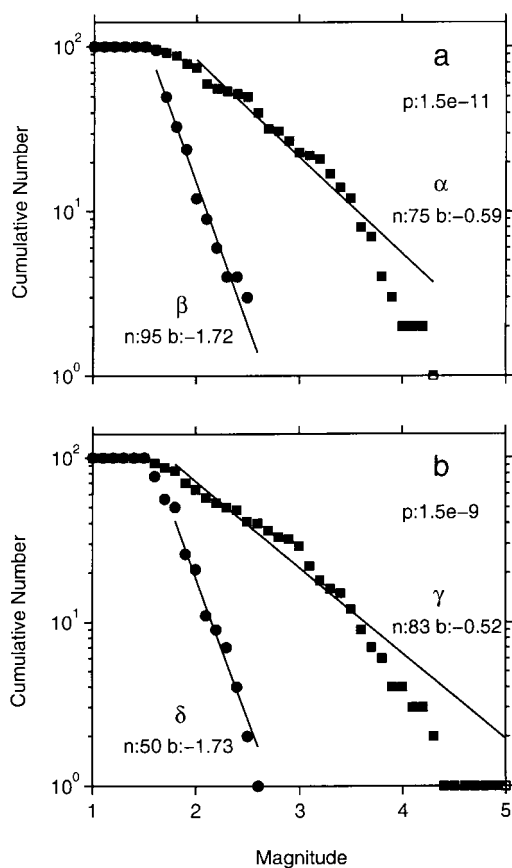


Fig. 7. Examples of frequency magnitude distributions for different sub-volumes of the South Flank. The locations of the volumes identified as  $\alpha$ ,  $\beta$ ,  $\gamma$ , and  $\delta$  are defined in Figs. 4 and 5. The number of events used for the calculation of the probability,  $p$ , are given as  $n$ .

seen in Fig. 6. So far, we have not found this kind of image at distances of several kilometers away from other volcanoes.

## 5. Discussion and conclusions

A normal pattern of  $b$ -value as a function of depth (Eaton et al., 1970; Wyss, 1973; Mori and Abercrombie, 1997; Wiemer and Wyss, 1997; Gerstenberger et al., 2000) is exhibited by the crust beneath Kaoiki-Hilea (Figs. 3b, 4b). We interpret this to mean that there is nothing special about the distribution of cracks, or the state of stress, in Hawaiian crust, in general. However, the anomalously high  $b$ -values beneath Kilauea's South Flank (Figs. 3a, 4a, 5 and 6) show that *there* the crust at intermediate depth and close to the East Rift zone produces many more small earthquakes than large ones, when compared to normal crust. Or, alternatively stated, these volumes seldom produce moderately large earthquakes ( $M > 3$ ), yet numerous little ones (Fig. 7).

### 5.1. The physical mechanism of $b$ -value anomalies

The preponderance of small events in rock-failure experiments in the laboratory can be due to increased heterogeneity of the rock samples (Mogi, 1962) or due to lower ambient stress (Scholz, 1968), which can be described as a state of higher heterogeneity of stress within the sample. This is true because, at low ambient stress, the local stress level varies between very low values and the breaking strength, whereas at high ambient stress the amplitude of this variation ranges from moderate values to the same maximum at the breaking strength. Unfortunately, there are no clues that would allow us to choose material heterogeneity or low stress (high-pore pressure) as the mechanism that perturbs  $b$  to high values near magma chambers. Both explanations seem equally plausible: Around magma chambers the crust is likely to be more extensively cracked than elsewhere (heterogeneous), but high pore pressure is also probable. It may be that both factors contribute to the high  $b$ -values observed. Along faults, far from magmatic activity, it seems that a choice of a mechanism is possible: Along the San Andreas fault segment, where aseismic creep occurs, for example, low stresses are the likely explanation for high  $b$ -values ( $b > 1.3$ ) (Amelung and King, 1997;

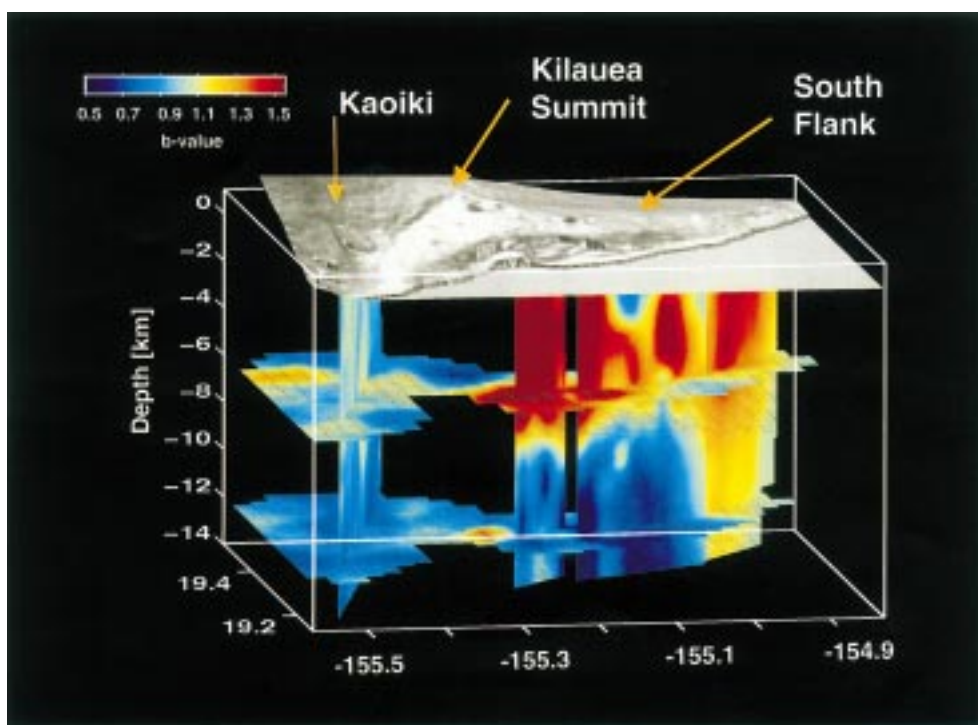


Fig. 8. Three-dimensional image of the  $b$ -values beneath Kilauea's South Flank and the Kaoiki-Hilea region. In this map of strongly varying mean magnitude, the earthquakes directly below the rift zones and the caldera of Kilauea are not used. The  $b$ -values are normal to low in the Kaoiki area and at depths greater than about 8 km beneath the South Flank.  $b$ -values are anomalously high ( $b > 1.3$ ) at 4–7 km depths in the South Flank, varying in intensity along strike. We interpret these high  $b$ -values (absence of intermediate size earthquakes) to indicate that a series of magma bodies at intermediate depth may exist beneath the ERZ.

Wiemer and Wyss, 1997), and high stresses in asperities probably cause the low  $b$ -values ( $b < 0.6$ ) observed there (Wiemer and Wyss, 1997).

In Hawaii, the best-developed and probably relatively smooth fault is the sub-horizontal to slightly island-dipping decollement plane at about 10 km depth. Hence, we assume that the smoothness (relative homogeneity) of the decollement plane favors larger ruptures.

Within Kilauea's South Flank, above the decollement plane, some earthquakes occur on thrust planes not favorably oriented with respect to the local stress tensor (Gillard et al., 1995). From this evidence, one might conclude that low stresses are not an acceptable explanation for the high  $b$ -values observed. However, it is probable that high pore pressures in the South Flank could contribute to this high  $b$  anomaly. In the Kaoiki area, the pore pressure is likely to reach 90% of the lithostatic pressure (Wyss et al., 1992).

This mechanism may be at work in the South Flank also.

### 5.2. The location of $b$ -value anomalies relative to volcanic structures

Regardless of the physical mechanism responsible, we propose, based on the similarity of this pattern with the one we observed beneath other volcanoes (Wiemer and McNutt, 1997; Wyss et al., 1997; Wiemer et al., 1998; Power et al., 1998; Murru et al., 1999), that the high  $b$ -value anomalies indicate that active magma chambers are nearby. Since Kilauea's East Rift zone (ERZ) lies adjacent to the South Flank volume with anomalously high  $b$ -values, and since the  $b$ -values are highest close to the rift zone (Fig. 5), we infer that active magma reservoirs (or concentrated dike formations) beneath the ERZ cause these anomalies (Fig. 9).

The most obvious pattern we observe is that  $b$ -values at intermediate depths (4–7 km) are anomalously high (Figs. 3–6 and 8). The second pattern we notice is that the  $b$ -values vary along the strike of the rift zone (Figs. 6a and 8) and form three major and two or three minor anomalies. The rift locations where local shallow magma reservoirs have been proposed are marked with triangles in Fig. 6. In map view, high  $b$ -value anomalies are seen adjacent to these locations. However, these magma bodies are believed to be small and at shallow depths of about 1–4 km, whereas the  $b$ -value anomalies are at depths deeper than 4 km (Figs. 5 and 6a). The top 4 km of the South Flank contains so few earthquakes that the  $b$ -value image is only sketchy and therefore not shown in Fig. 6.

The magma reservoirs in the rift are revealed as centers of inflation and deflation, as sources of eruptions of stored and differentiated magma, and by seismicity patterns. Magnetic anomalies (peaks larger than 600 nT; Kauahikaua, 1993) and self-potential anomalies (peaks larger than 1.0 v; Zablocki, 1976; Kauahikaua, 1993; Zablocki and Koyanagi, 1979) are also geophysical indicators of possible magma concentration.

Four of the six published magma reservoirs coincide closely (within 3 km) with magnetic and/or self-potential anomalies. These reservoirs may be major and persistent features, and are plotted with solid triangles in Fig. 6. They also are the reservoirs that correlate strongly with the major  $b$ -value anomalies.

The strongest  $b$ -value anomaly (near longitude  $-155.22^\circ$ ) coincides with one of the structurally most significant parts of the rift zone, the Hiiaka-Pauahi magma reservoir, located where the rift zone joins the extensional Koa'e Fault Zone and where the rift bends eastward. This reservoir was a starting point of intrusions as revealed by earthquakes that migrated both up- and down-rift and as an aseismic zone within the rift (Klein et al., 1987, Fig. 43.100).

Swanson et al. (1976b) and Jackson et al. (1975) proposed there was another reservoir under Makaopuhi, based on uplift and dilation near the eventual Mauna Ulu eruption site. The Makaopuhi reservoir has a magnetic anomaly and may account for the deformation centers reported by Dvorak et al. (1983). Again, we see a clear  $b$ -value anomaly adjacent to this location in the South Flank at depth between 4 and 7 km (Fig. 9).

A third reservoir is believed to be active under the Puu Kamoamo-a-to-Kalalua middle section of the rift ( $-155.05^\circ$  to  $-154.95^\circ$ ). It underlies the current Puu Oo eruption and accumulated magma before the start of the eruption (Wolfe, 1988, p. 178). Klein et al. (1987, p. 1179 and Figure 43-100) and Wilson and Head (1988) drew the reservoir not as a point but as a body extended along the rift because of the geometry of inflationary tilt vectors before the eruption (Wolfe, 1988, Fig. 6.6). This extended reservoir and the lack of a localized magnetic or self-potential anomaly may account for the observation that the  $b$ -value anomaly is less intense at this location but extends adjacent to an 8 km section of the rift zone (Fig. 6).

The  $b$ -values between  $-155.05$  and  $-154.95^\circ$  are high near the rift but do not show a concentrated anomaly. Moore (1983) proposed a reservoir under Heiheiahulu using the differentiation of erupted lava at this site. Based on the dispersed  $b$ -value anomaly and other anomalies in this section of the rift, we propose that magma storage

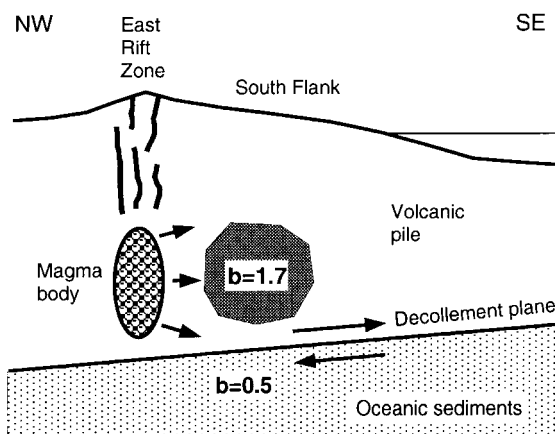


Fig. 9. Schematic outline of the distribution of  $b$ -values in Kilauea's South Flank in a cross section perpendicular to the east rift zone. The anomalously high  $b$ -values of  $b = 1.7$  (overabundance of small earthquakes) at intermediate depths (4–7 km) and near the rift zone are interpreted to be due to the presence of an active magma chamber at depth between 4 and 8 km, which generates a heterogeneous, intensely cracked crust. The anomalously low  $b$ -values of  $b = 0.5$  (preponderance of larger earthquakes) at  $9 \pm 1$  km depth are interpreted as associated with the near horizontal decollement plane over which the volcanic edifice is sliding out to sea, away from the rift and caldera of Kilauea.

in the middle ERZ is not concentrated into a large or persistent reservoir.

A third major  $b$ -value anomaly is noticeable in Fig. 6 at the farthest point down rift for which we have data (near longitude  $-154.91^\circ$ ). This  $b$ -value anomaly is adjacent to a magma reservoir proposed by Moore (1983) under the Puu Kaliu cone based primarily on differentiated lava chemistry. Unfortunately, we have less confidence in the earthquake data in this area because the seismicity is relatively sparse and the location precision and detection threshold of the network is poorer than in the area to the west.

The  $b$ -value anomalies, when projected onto the axis of the East Rift zone, correlate well with magma reservoirs. We favor the interpretation of magma reservoirs facilitating and feeding dike growth, and causing dense crack concentrations that are expressed by magnetic, self-potential and  $b$ -value anomalies.

The depth extent of the rift reservoirs is unknown because surface deformation measurements are most sensitive to the shallow (2–4 km) parts of the reservoirs, and earthquakes within the rift zone are primarily generated by magma movement and intrusions in the upper 4 km. The simplest explanation of our observation of anomalously high  $b$ -values near the five suspected shallow magma reservoirs, but at depths between 4 and 7 km, is the assumption that the reservoirs have roots that extend to at least 7 km depth.

### 5.3. Correlation with tomography

Our result that the crust at intermediate depth in the South Flank is anomalous, in contrast to the crust in the Kaoiki area correlates to a large degree with P-wave anomalies (Okubo et al., 1997). Between 3 and 5 km and below 7 km the P-velocities are above 6 km/s. In the range of 5–7 km the velocities are reported to be lower (about 5.5 km/s) than above and below these depths in most of southern Hawaii, but least so in the Kaoiki area, where they are still above 6 km/s. In the part of the South Flank that we have analyzed, the volumes with the strongest P-wave anomalies (5 km/s) correlate with the strongest  $b$ -value anomalies near  $19.32^\circ$ – $155.23^\circ$  and  $19.33^\circ$ – $155.17^\circ$ . A narrow zone of normal values separates both  $b$ -value and P-wave anomalies. This coincidence of high  $b$ -value with low velocity supports

the interpretation that the crust at intermediate depth in the South Flank is highly fractured.

### 5.4. The physical state of Kilauea's South Flank

The proposal that magma exists at depths below 4 km beneath the East Rift zone along most of its length (Ryan, 1988; Delaney et al., 1990) was controversial because the effects of the shallow magma are more obvious. At depths greater than 4 km, the crust beneath the rift zone is not sufficiently brittle to generate earthquakes. Thus, magma movements cannot be directly tracked by seismicity. Nevertheless, the deep-magma model has more recently become accepted by some (Fiske et al., 1993) based on the timing of eruptions. Our data can be interpreted as mapping the collateral pore-fluid pressure effects or high crack density, also supported by P-wave tomography, induced by a magma body between 3 and 7 km depth (Figs. 5, 8 and 9), and reaching from Kilauea summit at least 40 km down the East Rift zone (Figs. 6 and 8).

The depth estimates of magma reservoirs based on our method closely agreed with independent estimates for eight such reservoirs at five other volcanoes (Wiemer and McNutt, 1997; Wyss et al., 1997; Wiemer et al., 1998; Murru et al., 1999). However, Kilauea's South Flank is similar to, but also different from the list of other cases in which we found that high  $b$ -value anomalies appear to map magma chambers (Mt. St. Helens, Mt. Spurr, off-Ito, Long Valley, Mt. Etna, Mt. Redoubt). In these other cases, the  $b$ -value anomalies were located almost directly beneath the surface eruption sites, and the dimensions of the anomalies were typically about 2 km. The anomalous volume in the South Flank, however, extends with varying intensity all along the seismogenic length of the South Flank (about 40 km) and 5–8 km in the direction perpendicular to the strike of the rift zone (Figs. 5 and 6). The factor that is most different at Kilauea, compared to other volcanoes, is the mobility of its South Flank. It seems reasonable to explain the deep penetration of the  $b$ -value anomalies into the South Flank by the transport of the seismogenic volume by about 10 cm/year in a SS-Westerly direction, away from the ERZ.

One might argue that the observed 5–8 km width of the high  $b$ -value anomaly (Figs. 5, 6 and 9) may be a

result of the high magma production and eruption frequency of Kilauea volcano. However, the individual eruption centers along the ERZ, which correlate with the *b*-value anomalies, do not erupt more frequently than some of the other volcanoes we analyzed in previous papers. Also, if the eruption rate of Kilauea were the only cause of the deep penetration of the anomalies, the same would have to be observed for the Kaoiki area, which is not the case. Thus, we discount high eruption rate as an explanation of Kilauea's larger *b*-value anomalies compared to other volcanoes.

The *b*-value anomalies can physically be explained in two ways: by high pore-fluid pressures or by excessive heterogeneity. If the South Flank is permeated by pore-fluids (M. Ryan, personal communication) trapped in sealed pockets, anomalously high pore pressures could build up and give rise to high *b*-values. This explanation is plausible because in Long Valley we demonstrated that an intrusion altered *b*-values from average to high during a period of less than one month and to distances of 3 km from the volume penetrated by the magma (Wiemer et al., 1998).

An alternative model, assuming that unusually strong heterogeneity contributes to the high *b*-value anomaly, could be constructed. The South Flank is geodetically observed to move out to sea, away from the East Rift zone, where intrusions provide the pushing hand (Swanson et al., 1976a; Dieterich, 1988; Delaney et al., 1990; Owen et al., 1995; Gillard et al., 1995). Thus, much of the volcanic edifice of any part of the South Flank was originally generated along the East Rift zone, similar to ocean floor being created by spreading at the ridges. In this process the rift zone itself moves away from the buttressed edifice of the island of Hawaii at less than the double 'spreading rate.' The moving rift leaves behind the gravity and magnetic signatures as reported by Kauahikaua (1993), which indicate a 'fossil' rift under the flank north of the East Rift Zone. The moving rift is tied to a fixed magma source (Kilauea Caldera), which probably accounts for the bend of the growing rift zone (Fiske and Jackson, 1972; Ryan, 1988).

It is likely that the new crust generated at the rift is cracked extensively during its infancy, while still near the active magma body. If this new, cracked and heterogeneous crust travels southward and becomes

part of the South Flank, retaining its crack distribution, then the South Flank, even several km away from the rift, may be more heterogeneous than regular crust, leading to anomalously high *b*-values and anomalously low P-velocities (Okubo et al., 1997). Thus, one may propose that the major magma reservoirs along the ERZ leave a track at depth within the moving flank revealed by a deficiency of large earthquakes relative to small ones.

The association of South Flank *b*-value anomalies with rift zone magma reservoirs and magnetic and self-potential anomalies argues that the reservoirs are persistent features. Both the crack and pore pressure models involve a physical change in the South Flank that cannot alter as quickly as stress geometry, for example. Regardless of the choice of explanation of the high *b*-values in the South Flank, this crustal volume is unusual and different from other seismogenic crust in Hawaii and California.

Although the interpretation of *b*-value anomalies is non-unique, and we do not have enough experience with these newly discovered small-scale anomalies to know with certainty which among these (or other) physical explanations may be correct, it is clear that much information is contained in the pattern of the distribution of small and large earthquakes. The simplest explanation of the high *b*-value anomalies in Kilauea's South Flank is that the five suspected shallow magma reservoirs have roots to 7 km depth. Thus, we envision a model of the deep rift zone in which a series of magma bodies are strung along the rift zone like a chain of sausage links. Fig. 9 depicts one of the locations in which a local reservoir reaches a significant thickness, and such reservoirs may be connected to each other, up and down the rift, by narrower dikes. Our model is similar to that of magma intruding by dikes proposed for different volcanoes by Eichelberger and Izbekov (2000).

In spite of the complications discovered in this *b*-value analysis of Kilauea's South Flank, there are many similarities with the case histories of the other volcanoes we have studied, and the correlation of high *b*-value anomalies with magma reservoirs is confirmed.

#### Acknowledgements

We thank M. R. Ryan and G. Saccorotti for

suggestions and rewording in reviews that led to many improvements and T. Wright for helpful comments. This work was supported by NSF under grant number EAR-9614783, the Wadati endowment at the Geophysical Institute of the University of Alaska, Fairbanks, and a fellowship from the overseas research scholarship fund number 8-waka-190 by the Ministry of Education, Science, Sports and Culture, Japan for K. N. This paper is contribution number 1133 of the Geophysical Institute of ETH Zurich.

## References

- Aki, K., 1965. Maximum likelihood estimate of  $b$  in the formula  $\log N = a - bM$  and its confidence limits. *Bull. Earthq. Res. Inst.* 43, 237–239 (University of Tokyo).
- Amelung, F., King, G., 1997. Earthquake scaling laws for creeping and non-creeping faults. *Geophys. Res. Lett.* 24, 507–510.
- Crosson, R.S., Endo, E., 1982. Focal mechanisms and locations of earthquakes in the vicinity of the 1975 Kalapana earthquake aftershock zone 1970–1979: implications for tectonics of the South Flank of Kilauea volcano. *Tectonics* 1, 495–542.
- Delaney, P.T., Fiske, R.S., Miklius, A., Okamura, A.T., Sato, M.K., 1990. Deep magma body beneath the summit and rift zones of Kilauea Volcano, Hawaii. *Science* 247, 1311–1316.
- Dieterich, J.H., 1988. Growth and persistence of Hawaiian volcanic rift zones. *J. Geophys. Res.* 93, 4258–4270.
- Dvorak, J.J., Okamura, A.T., Dieterich, J.H., 1983. Analysis of surface deformation data, Kilauea Volcano, Hawaii, October 1966 to September 1970. *J. Geophys. Res.* 88, 9295–9304.
- Dvorak, J.J., Okamura, A.T., English, T.T., Koyanagi, R.Y., Nakata, T.S., Sako, M.K., Tanigawa, W.T., Yamashita, K.M., 1986. Mechanical response of the south flank of Kilauea volcano, Hawaii, to intrusive events along the rift systems. *Tectonophysics* 124, 193–209.
- Dzurisin, D., Koyanagi, R.Y., English, T.T., 1984. Magma supply and storage at Kilauea volcano, Hawaii. *J. Volcanol. Geotherm. Res.* 21, 177–206.
- Eaton, J., O'Neil, M., Murdock, J., 1970. Aftershocks of the 1966 Parkfield-Cholame, California, earthquake: a detailed study. *Bull. Seismol. Soc. Am* 60, 1151–1197.
- Eichelberger, J.C., Izbekov, P.E., 2000. Eruption of andesite triggered by dyke injection: contrasting cases at Karymsky volcano, Kamtchatka and Mt. Katmai, Alaska. *Phil. Trans. R. Soc. London A* 359, 1465–1485.
- Fiske, R.S., Jackson, E.D., 1972. Orientation and growth of Hawaiian volcanic rifts: The effect of regional structure and gravitational stresses. *Proc. R. Soc. London, Ser. A* 329, 299–326.
- Fiske, R.S., Swanson, D.A., Wright, T.L., 1993. A model of Kilauea volcano's rift-zone magma system. *EOS* 74, 646.
- Gerstenberger, M., Wiemer, S., Giardini, D., 2000. A systematic test of the hypothesis that the  $b$  value varies with depth in California. *Geophys. Res. Lett.* 27, in press.
- Gillard, D., Wyss, M., Okubo, P., 1995. Stress and strain tensor orientations in the south flank of Kilauea, Hawaii, estimated from fault plane solutions. *J. Geophys. Res.* 100, 16 025–16 042.
- Gillard, D., Rubin, A.M., Okubo, P., 1996. Highly concentrated seismicity caused by deformation of Kilauea's deep magma system. *Nature* 384, 343–346.
- Got, J.L., Frechet, J., Klein, F.W., 1994. Deep fault plane geometry inferred from multiplet relative relocation beneath the south flank of Kilauea. *J. Geophys. Res.* 99, 15 375–15 386.
- Gutenberg, R., Richter, C.F., 1944. Frequency of earthquakes in California. *Bull. Seismol. Soc. Am* 34, 185–188.
- Habermann, R.E., 1983. Teleseismic detection in the Aleutian Island arc. *J. Geophys. Res.* 88, 5056–5064.
- Hardee, H.C., 1987. Heat and mass transport in the east-rift-zone magma conduit of Kilauea volcano. In: Decker, R.W., Wright, T.L., Stauffer, P.H. (Eds.), *Volcanism in Hawaii*. US Geological Survey Professional Paper 1350, pp. 1471–1486.
- Hill, D.P., Zucca, J.J., 1987. Geophysical constraints on the structure of Kilauea and Mauna Loa volcanos and some implications for seismomagmatic processes. R.W. Decker, T.L. Wright, P.H. Stauffer, (Eds.), *Volcanism in Hawaii*. US Geol. Surv. Prof. Pap. 1350, pp. 903–918.
- Ishimoto, M., Iida, K., 1939. Observations of earthquakes registered with the microseismograph constructed recently. *Bull. Earthq. Res. Inst.* 17, 443–478 (University of Tokyo).
- Jackson, D.B., Swanson, D.A., Koyanagi, R.Y., Wright, T.L., 1975. The August and October 1968 east rift eruptions of Kilauea volcano, Hawaii. US Geological Survey Professional Paper 890.
- Kauahikaua, J., 1993. Geophysical characteristics of the hydrothermal systems of Kilauea volcano, Hawaii. *Geothermics* 22, 271–299.
- Klein, F.W., 1981. A linear gradient crustal model for south Hawaii. *Bull. Seismol. Soc. Am* 71, 1503–1510.
- Klein, F.W., Koyanagi, R.Y., Nakata, J.S., Tanigawa, W.R., 1987. The Seismicity of Kilauea's magma system. In: *Volcanism in Hawaii*. US Geological Survey Professional Paper 1350, pp. 1019–1186.
- Lahaie, F., Grasso, J.R., 1999. Loading rate impact on fracturing pattern: lessons from hydrocarbon recovery, Lacq gas field, France. Submitted for publication.
- Mogi, K., 1962. Magnitude–frequency relation for elastic shocks accompanying fractures of various materials and some related problems in earthquakes. *Bull. Earthq. Res. Inst.* 40, 831–853 (University of Tokyo).
- Moore, R.B., 1983. Distribution of differentiated tholeiitic basalts on the lower east rift zone of Kilauea Volcano, Hawaii: a possible guide to geothermal exploration. *Geology* 11, 136–140.
- Mori, J., Abercrombie, R.E., 1997. Depth dependence of earthquake frequency–magnitude distributions in California: Implications for the rupture initiation. *J. Geophys. Res.* 102, 15 081–15 090.
- Murru, M., Montuori, C., Wyss, M., Privitera, E., 1999. The location of magma chambers at Mt. Etna, Italy, mapped by  $b$ -values. *Geophys. Res. Letts.* 26, 2553–2556.
- Ogata, Y., Utsu, T., Katsura, K., 1995. Statistical features of foreshocks in comparison with other earthquake clusters. *Geophys. J. Int.* 121, 233–254.
- Okubo, P.G., Benz, H.M., Chouet, B., 1997. Imaging the crustal magma source beneath Mauna Loa and Kilauea volcanoes, Hawaii. *Geology* 25, 867–870.

- Owen, S., Segall, P., Freymueller, J., Miklius, A., Denlinger, R., Arnadotir, T., Sako, M., Buergermann, R., 1995. Rapid deformation of the south flank of Kilauea volcano, Hawaii. *Science* 267, 1328–1332.
- Power, J.A., Wyss, M., Latchman, J.L., 1998. Spatial variations in frequency–magnitude distribution of earthquakes at Soufriere Hills volcano, Montserrat, West Indies. *Geophys. Res. Lett.* 25, 3653–3656.
- Reasenber, P.A., 1985. Second-order moment of Central California Seismicity. *J. Geophys. Res.* 90, 5479–5495.
- Ryan, M.P., 1988. The mechanics and the three-dimensional internal structure of active magmatic systems: Kilauea volcano, Hawaii. *J. Geophys. Res.* 93, 4213–4248.
- Scholz, C.H., 1968. The frequency–magnitude relation of microfracturing in rock and its relation to earthquakes. *Bull. Seismol. Soc. Am* 58, 399–415.
- Swanson, D.A., Duffield, W.A., Fiske, R.S., 1976a. Displacement of the south flank of Kilauea volcano: the result of forceful intrusion of magma into the rift zones. *U.S. Geol. Surv. Prof. Pap.* 963, pp. 1–39.
- Swanson, D.A., Jackson, D.B., Koyanagi, R.Y., Wright, T.L., 1976b. The February 1969 east rift eruption of Kilauea volcano, Hawaii. *US Geological Survey Professional Paper* 891.
- Urbancic, T.I., Trifu, C.I., Long, J.M., Young, R.P., 1992. Space–time correlations of *b*-values with stress release. *Pure Appl. Geophys.* 139, 449–462.
- Utsu, T., 1965. A method for determining the value of *b* in a formula  $\log n = a - bM$  showing the magnitude frequency for earthquakes. *Geophys. Bull. Hokkaido Univ.* 13, 99–103.
- Utsu, T., 1992. On seismicity, in *Mathematical Seismology (VII)*, Cooperative Research Report 34, Institute for Statistical Mathematics, Tokyo, pp. 139–157.
- Warren, N.W., Latham, G.V., 1970. An experimental study of thermally induced microfracturing and its relation to volcanic seismicity. *J. Geophys. Res.* 75, 4455–4464.
- Wiemer, S., 1996. Analysis of seismicity: new techniques and case studies. Dissertation thesis, University of Alaska, Fairbanks, Alaska.
- Wiemer, S., Benoit, J., 1996. Mapping the *b*-value anomaly at 100 km depth in the Alaska and New Zealand subduction zones. *Geophys. Res. Lett.* 23, 1557–1560.
- Wiemer, S., Katsumata, K., 1999. Spatial variability of seismicity parameters in aftershock zones. *J. Geophys. Res.* 104, 13 135–13 151.
- Wiemer, S., McNutt, S., 1997. Variations in frequency–magnitude distribution with depth in two volcanic areas: Mount St. Helens, Washington, and Mt. Spurr, Alaska. *Geophys. Res. Lett.* 24, 189–192.
- Wiemer, S., Wyss, M., 1997. Mapping the frequency–magnitude distribution in asperities: An improved technique to calculate recurrence times? *J. Geophys. Res.* 102, 15 115–15 128.
- Wiemer, S., Zuniga, R.F., 1994. ZMAP — a software package to analyze seismicity. *EOS, Transactions, Fall Meeting, AGU* 75, 456.
- Wiemer, S., McNutt, S.R., Wyss, M., 1998. Temporal and three-dimensional spatial analysis of the frequency–magnitude distribution near Long Valley caldera, California. *Geophys. J. Int.* 134, 409–421.
- Wilson, L., Head, J.W., 1988. Nature of local magma storage zones and geometry of conduit systems below basaltic eruption sites: Puu Oo, Kilauea East Rift, Hawaii, example. *J. Geophys. Res.* 93, 14 785–14 792.
- Wolfe, E.W. (Ed.), 1988. The Puu Oo eruption of Kilauea Volcano, Hawaii: Episodes 1 through 20, January 3, 1983 through June 8, 1984. *US Geological Survey Professional Paper* 1463.
- Wyss, M., 1973. Towards a physical understanding of the earthquake frequency distribution. *Geophys. J. R. Astronom. Soc.* 31, 341–359.
- Wyss, M., 1988. A proposed source model for the great Kau, Hawaii, earthquake of 1868. *Bull. Seismol. Soc. Am* 78, 1450–1462.
- Wyss, M., Gillard, D., Liang, B., 1992. An estimate of the absolute stress tensor in Kaoiki, Hawaii. *J. Geophys. Res.* 97, 4763–4768.
- Wyss, M., Shimazaki, K., Wiemer, S., 1997. Mapping active magma chambers by *b*-value beneath the off-Ito volcano, Japan. *J. Geophys. Res.* 102, 20 413–20 422.
- Wyss, M., Schorlemmer, D., Wiemer, S., 1999. Mapping asperities by minima of local recurrence time: the San Jacinto-Elsinore fault zones, *J. Geophys. Res.* 105, 7829–7844.
- Zablocki, C.J., 1976. Mapping thermal anomalies on an active volcano by the self-potential method. Kilauea, Hawaii. *UN Symposium on the development and use of geothermal resources*, vol. 2, pp. 1299–1309.
- Zablocki, C.J., Koyanagi, R.Y., 1979. An anomalous structure in the lower east rift zone of Kilauea Volcano, Hawaii, inferred from geophysical data, Hawaii, *Symposium on intraplate volcanism and submarine volcanism abstract volume*, Hilo, Hawaii, 16–22 July, p. 177.
- Zuniga, R., Wyss, M., 1995. Inadvertent changes in magnitude reported in earthquake catalogs: Influence on *b*-value estimates. *Bull. Seismol. Soc. Am* 85, 1858–1866.
- Zuniga, F.R., Wiemer, S., 1999. Seismicity patterns: are they always related to natural causes? *Pure Appl. Geophys.* 153, 713–726.